Time-dependent adaptive mesh refinement for 3D forward modelling of transient electromagnetic fields in volcanic environments including topography

C. Schneider[1], K. Spitzer[1] and M. Hort[2]
[1]TU Bergakademie Freiberg, Germany, carolin.schneider@geophysik.tu-freiberg.de,
klaus.spitzer@geophysik.tu-freiberg.de
[2]Universität Hamburg, matthias.hort@uni-hamburg.de

SUMMARY

Numerical forward modelling of transient electromagnetic (TEM) fields in topographically demanding terrain is a rather challenging task but inevitable to identify reasonable measurement configurations and to correctly interpret acquired field data when investigating mountainous regions. Since the propagating electromagnetic fields change with time and space, an adaptively refined grid would ideally be time-dependent, too. Generating large unstructured tetrahedral grids tailored manually to each specific time-step is, however, very time consuming. Moreover, the system matrix also changes with time causing additional numerical work in the solution process. We tackle both problems by using a very efficient Krylov-subspace method which projects the system matrix onto a low-dimensional space and, therefore, enables us to evaluate the solution for any given time. Additionally, we propose an adaptive approach including hanging edges within our modelling domain. With this, an initial mesh is refined according to the requirements of the propagating electromagnetic field. The development is driven by the application of TEM at volcanic sites. There is an enormous volcanological interest in magmatic pathways and hydrothermal systems within volcanic structures aiming to understand processes occurring prior to a volcanic eruption. Therefore, we apply our TEM simulation routine to a model of Stromboli volcano, Italy, created from a digital elevation model (DEM).

Keywords: modelling, transient electromagnetics, Krylov subspace, adaptive mesh refinement

INTRODUCTION

Numerical modelling using finite elements (FE) is a common tool in geoelectromagnetics. Its accuracy is strongly affected by the underlying mesh as has been vividly demonstrated by the work of Schwarzbach (2009). Several approaches exist to generate an appropriate mesh: Usually, an experienced user sets up an *a-priori* refined mesh with high resolution in the vicinity of the receiver and transmitter locations. On the other hand, *a-posteriori* error estimators are used to quantify the discretization error associated with a specific mesh, which has been proposed by, e.g., Ren et al (2013). In frequency-domain modelling the fineness of the mesh is also related to the frequency. Consequently, the mesh has to be a function of time in time-domain modelling. We therefore suggest to create a series of meshes adapted to the individual time step. This is usually prohibitively expensive but becomes feasible with the Krylov subspace technique we are using here. In order to tailor the mesh to specific times in the TEM forward problem, we use an extension of the hanging node approach on Nédélec elements. The refinement routine guided by an error indicator can be applied to a DEM derived topographic model. Here, we apply our technique to a model of Stromboli volcano, Italy.

MATHEMATICAL BACKGROUND

TEM utilizes the turn-off of a DC current in a usually square loop on the Earth's surface to induce eddy currents in the underground decaying in intensity and expanding in space. They can be modeled by solving the field equation for the electric field $\mathbf{E}$ derived from Maxwell's equations. The TEM measurand, a normalized temporal variation of the magnetic flux density at the Earth's surface, is then extracted using Ampère's law $\partial_t \mathbf{B} = \nabla \times \mathbf{E}$.

Electric field equation

We state the time domain formulation of transient electromagnetic induction in terms of the electric field $\mathbf{E}$ as an initial-boundary value problem (e.g. Afanasjew et al, 2013; Börner et al, 2008, 2015)

$$\nabla \times (\mu^{-1} \nabla \times \mathbf{E}) + \sigma \partial_t \mathbf{E} = \mathbf{0} \quad \text{on } \Omega \times \mathbb{R}_+, \tag{1a}$$
$$\mathbf{E}|_{t=0} = \sigma^{-1} \mathbf{j} \quad \text{on } \Omega, \tag{1b}$$
$$\mathbf{n} \times \mathbf{E} = \mathbf{0} \quad \text{on } \partial\Omega \times \mathbb{R}_+, \tag{1c}$$

where $\mu = \mu_0$ represents the magnetic permeability of free space, $\sigma = \sigma(\mathbf{x})$ the spatially varying electrical conductivity, and $\mathbf{j}$ the source current density associated with a current shut-off at time t_0.
The spatial discretization on an unstructured tetrahedral grid using curl-conforming Nédélec elements yields an ODE initial value problem reading

$$\partial_t \mathbf{u}(t) + A\mathbf{u}(t) = \mathbf{0}, \quad t \in \mathbb{R}_+, \tag{2a}$$
$$\mathbf{u}(0) = \mathbf{b}, \tag{2b}$$

where $\mathbf{u}$ is the coefficient vector of the FE approximation of $\mathbf{E}$ with respect to the Nédélec basis at times $t > 0$ and $\mathbf{b}$ denotes the vector of initial values. The matrix *A* includes both the spatial approximation of the curl-curl operator and the spatially varying conductivity $\sigma(\mathbf{x})$.
Now, we find a solution to Equation 2 using a matrix exponential function

$$\mathbf{u}(t) = e^{-tA}\mathbf{b}, \tag{3}$$

which can be evaluated by developing a rational Arnoldi approximation at any given time $t > 0$ (Afanasjew et al, 2008; Börner et al, 2015).

Hanging edge approach

Adaptive mesh refinement using hanging nodes for octree finite volume discretizations has already been described by, e.g., Haber et al (2007). However, records are scarce for extending the approach to FE simulations based on Nédélec elements.
In Figure 1, a uniformly refined tetrahedron is depicted, where the original vertices enumerated 1-4 are indicated in black, while the vertices constructed within the refinement process are denoted by red numbers. When refining adjacent tetrahedra, new degrees of freedom are generated. However, if at least one adjacent tetrahedron is not refined, this causes hanging nodes and, consequently, hanging edges. Therefore, hanging edges only appear in the outskirts of a refined area, adjoint to the original (i.e. unrefined) mesh.

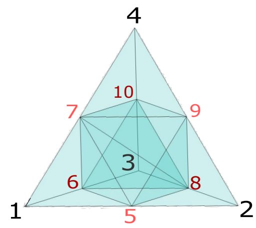

Figure 1: Uniformly refined tetrahedron, black digits enumerate the original vertices of the unrefined tetrahedron, red digits indicate vertices emerging from the refinement process.

Uniform refinement results in bisecting every single edge. Consequently, a set of geometrical constraints can be derived from the original, large edges ("parents") on the newly created, small edges ("children"), where edge $\vec{e}_{ij}$ denotes the edge linking vertices i and j (cf. Figure 1). The constraints derived from edge $\vec{e}_{12}$ read

$$\vec{e}_{15} = {}^1\!/\!_2\, \vec{e}_{12} \quad \text{and} \quad \vec{e}_{25} = {}^{-1}\!/\!_2\, \vec{e}_{12}. \tag{4}$$

Furthermore, the new edges emerging on the front facet of the depicted tetrahedron can be constrained using

$$\vec{e}_{57} = {}^1\!/\!_2\, \vec{e}_{24},\ \vec{e}_{59} = {}^1\!/\!_2\, \vec{e}_{14} \text{ and } \vec{e}_{79} = {}^1\!/\!_2\, \vec{e}_{12}. \tag{5}$$

In such a manner, each new edge can be constrained, except for an edge created inside the tetrahedron, such as edge $\vec{e}_{78}$ in Figure 1. Since the latter edge is embedded in the surrounding tetrahedra, it is a complete edge in the mathematical sense.
The stated constraints are mapped to the FE degrees of freedom on each refined tetrahedron and incorporated into the system matrix using the work of Abel and Shephard (1979).
Note, that the constrained degrees of freedom are a linearly interpolated and, consequently, do not yield additional information. The advantage of the hanging edge approach is the ability to refine a mesh straightforwardly without the need to treat hanging nodes at the level of grid generation.

RESULTS

In order to demonstrate the use of adaptive mesh refinement including hanging edges, we consider two applications common in 3D modelling: firstly, automatic refinement around the transmitter location and secondly, time-dependent tracking of the electric field in the subsurface.

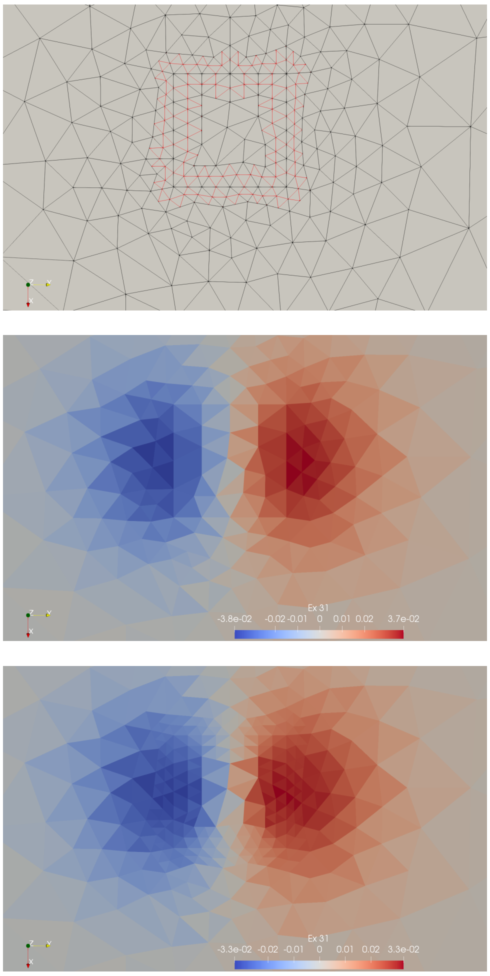

Figure 2: Unrefined (black) and refined (red) grid at the transmitter location (top) and E_x at time $t_1 = 10^{-6}\,\mathrm{s}$ in the unrefined (central) and refined mesh (bottom).

Homogeneous Halfspace

When modelling in the time domain, the fineness of the initial value condition severely affects the solution. Therefore, we automatically refine the region around the transmitter location within a homogeneous halfspace model with electrical conductivities $\sigma_{air} = 10^{-9}\,{}^{S}/_{\mathrm{m}}$ and $\sigma_{Earth} = 10^{-3}\,{}^{S}/_{\mathrm{m}}$ based on the solution E_x at time $t = 10^{-6}\,\mathrm{s}$ shown in Figure 2. In the uppermost panel, one can clearly observe hanging nodes where the refined mesh (red colour) borders the original mesh (black colour). As can be seen in the central and lowermost subplot, respectively, the solution on the fine mesh (lowermost figure) exhibits a smoother E_x distribution in contrast to the rather coarse solution on the original mesh (central figure). Due to the higher resolution in the initial step, the accuracy of the solution at later times is also raised.

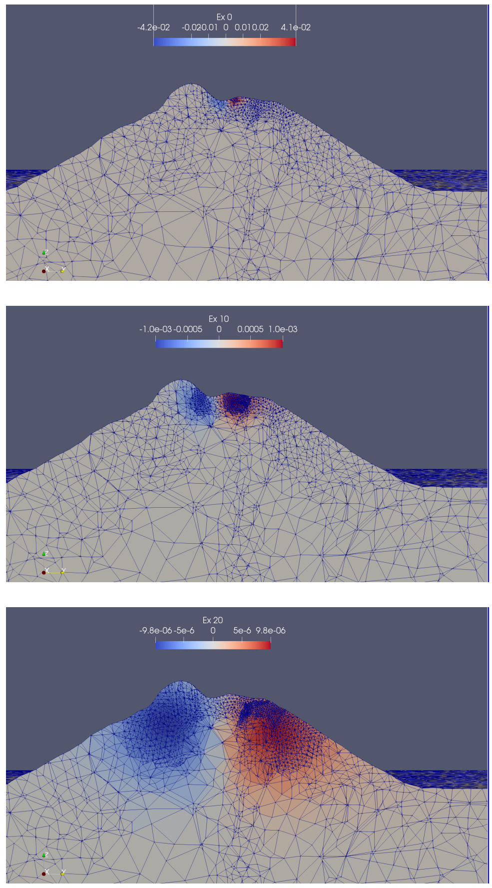

Figure 3: Tracking E_x in the underground using adaptive mesh refinement at times : $t_1 = 10^{-6}\,\mathrm{s}$, $t_2 = 10^{-5}\,\mathrm{s}$, $t_3 = 10^{-4}\,\mathrm{s}$ (from top to bottom).

Application to a DEM

As a second application for automatic adaptive refinement, we consider a homogeneous model of Stromboli volcano, Italy, derived from a DEM. Due to the steep topography, the electrical conductivities are set to $\sigma_{air} = 10^{-6}\,{}^{S}/_{\mathrm{m}}$ and $\sigma_{Earth} = 10^{-3}\,{}^{S}/_{\mathrm{m}}$

in order to maintain numerical stability at the Earth-air interface. An experienced user would generate a mesh with appropriate fineness in the vicinity of the receiver location, the transmitter location and at the Earth-air interface mapping the topography to a certain level of detailedness. However, additional refinement in the underground is necessary in the vicinity of conductivity anomalies and for accurately resolving the temporal behaviour of the electric field. In Figure 3, the tracking of E_x using the subset $\mathcal{T}_{ref}$ with

$$\mathcal{T}_{ref} = \{\ T \subset \Omega | E_x > 1/2 \max(E_x) \vee \\ E_x < 1/2 \min(E_x)\ \}$$

is visualized at times $t_1 = 10^{-6}\,\mathrm{s}$, $t_2 = 10^{-5}\,\mathrm{s}$ and $t_3 = 10^{-4}\,\mathrm{s}$. Note that, due to the nature of unstructured meshes, the interface of the clipped model may contain a variety of slices through tetrahedra which need not necessarily be triangular. The time-dependency of the underlying mesh is clearly visible, the fine regions follow the extrema of E_x. Apparently, the region, in which E_x is greater or less than half of its maximum/minimum value, respectively, widens with increasing time. This is in accordance with the diffussive nature of electromagnetic fields.

Conclusions

3D simulations of electromagnetic fields are highly useful to image electromagnetic fields in the underground. However, the accuracy of the results depends on the underlying mesh. In order to enhance the distribution of degrees of freedom we propose a strategy of time-dependent adaptive mesh refinement using hanging edges based on the extrema of the electric field. Future investigations will focus on the quantitative description of the refinement process.

Acknowledgments

The SRTMGL1 V003 data product was retrieved in July 2017 from the online Data Pool, courtesy of the NASA Land Processes Distributed Active Archive Center (LP DAAC), USGS/Earth Resources Observation and Science (EROS) Center, Sioux Falls, South Dakota,
https://lpdaac.usgs.gov/data access/data pool.

References

Abel JF, Shephard MS (1979) An algorithm for multipoint constraints in finite element analysis. International Journal for Numerical Methods in Engineering 14(3):464–467, DOI 10.1002/nme.1620140312

Afanasjew M, Eiermann M, Ernst OG, Güttel S (2008) Implementation of a restarted Krylov subspace method for the evaluation of matrix functions . Linear Algebra and its Applications 429:2293–2314

Afanasjew M, Börner RU, Eiermann M, Ernst OG, Spitzer K (2013) Efficient Three-Dimensional Time Domain TEM Simulation Using Finite Elements, a Nonlocal Boundary Condition, Multigrid, and Rational Krylov Subspace Methods. 5th International Symposium on Three-Dimensional Electromagnetics, May 7 - 9, 2013, Sapporo, Japan p 4p

Börner RU, Ernst OG, Spitzer K (2008) Fast 3-d simulation of transient electromagnetic fields by model reduction in the frequency domain using krylov subspace projection. Geophysical Journal International 173(3):766–780, DOI 10.1111/j.1365-246X.2008.03750.x

Börner RU, Ernst O, Güttel S (2015) Three-Dimensional Transient Electromagnetic Modeling Using Rational Krylov Methods. Geophys J Int 202(3)

Haber E, Heldmann S, Ascher U (2007) Adaptive finite volume method for distributed non-smooth parameter identification. Inverse Problems 23(4):1659–1676, DOI 10.1088/0266-5611/23/4/017

Ren Z, Kalscheuer T, Greenhalgh S, Maurer H (2013) A goal-oriented adaptive finite-element approach for plane wave 3-d electromagnetic modelling. Geophysical Journal International 194(2):700–718, DOI 10.1093/gji/ggt154

Schwarzbach C (2009) Stability of finite element solutions to Maxwell's equations in frequency domain. PhD thesis, TU Bergakademie Freiberg